Biocatalytic Polymerization of *p*-Cresol: An in-Situ NMR Approach To Understand the Coupling Mechanism

Sangrama K. Sahoo,[†] Wei Liu,[†] Lynne A. Samuelson,[‡] Jayant Kumar,[†] and Ashok L. Cholli*,[†]

Center for Advanced Materials, Departments of Chemistry and Physics, University of Massachusetts Lowell, Lowell, Massachusetts 01854, and Natick Soldier Center, U.S. Army Soldier and Biological Chemical Command, Natick, Massachusetts 01760

Received July 17, 2002; Revised Manuscript Received October 15, 2002

ABSTRACT: The nature of the initial coupling mechanism in the enzymatic polymerization of *p*-cresol was investigated by in-situ ^{1}H NMR spectroscopy in an aqueous−organic media. Two types of in-situ experiments were performed, in which the course of polymerization was monitored with (i) incremental additions of H_2O_2 to the reaction mixture in the NMR tube at a regular interval and (ii) a function of reaction time after a known amount of addition of H_2O_2. These experiments were used to understand the coupling mechanism at the very early stage of reaction and during the course of polymerization reaction. In the early stage of the polymerization, the reaction mixture contains monomer as a dominant fraction and a small concentration of low molecular weight oligomers such as dimer, trimers, etc. The analysis of the reaction mixture by 1D and 2D in-situ NMR methods suggests the ortho−ortho C−C coupling as the dominant coupling mechanism during the initial stage of the polymerization. The quantitative NMR analysis indicates that the relative consumptions of monomer and dimers are different at the early stage of polymerization; the consumption of dimer accelerates only after complete conversion of the monomer from the reaction mixture. The in-situ NMR analysis as a function of reaction time after addition of a known amount of H_2O_2 suggests the conversion of a quinonoid intermediate formed at the beginning from ortho−para C−C coupling, to a stable ketonic product (Pummerer's ketone). A gradual reduction of quinonoid structures and increase of Pummerer's ketone structures in the reaction mixture are monitored with time by in-situ NMR. Structural characterization of bulk polymer by multinuclei NMR spectroscopy and MALDI−TOF mass spectrometry indicates the formation of polymers (M_w 1230) and the dominance of ortho−ortho and ortho−para C−C coupled products. The polymers obtained from the reaction products contained a very low concentration of Pummerer's ketones, which may be chain ends.

Introduction

Enzymatic oxidative polymerization to produce phenolic polymers is of great commercial interest for the synthesis of polymers with novel structures and properties.[1−3] The ability of peroxidase enzymes to catalyze oxidative coupling of phenol and substituted phenols provides an alternate route for the synthesis of phenolic polymers, which have many applications in resin and coating technologies.[3,4] The heightened interest in this type of enzyme-based polymerization is mostly due to its environmental compatibility (*without the use of toxic chemicals*) and potential for producing industrial polymers in high yield.[5] Typically, peroxidase-catalyzed polymerization of phenol is carried out in the presence of H_2O_2, which acts as an oxidant, and the cycle of peroxidase involves a two-electron oxidation step and two one-electron reduction steps.[6] The free radicals of the monomer (substrate) in an aqueous or aqueous−organic solution undergo oxidative coupling to produce dimers and other oligomeric products. The successive oxidation and coupling of oligomers eventually resulted in the formation of high molecular weight polymers (polyphenols). In general, the main structure was estimated to be a mixture of phenylene and oxyphenylene units.[3,7] In addition, the regioselectivity of the final product can be controlled by the solvent composition, which yields a polymer with varying percentage of phenylene and oxyphenylene units.[8]

The basic structural difference between the phenol−formaldehyde-based polymer and the enzyme-catalyzed polyphenol is the absence of $-CH_2-$ groups in the latter. The aromatic rings are directly joined in the polyphenol obtained by enzymatic polymerization either through C−C or C−O−C bonding (C denotes the aromatic ring carbon). Direct C−C bond formation results in conjugation of the aromatic backbone and thus potential applications in electrooptics.[9,10] The properties of the polyphenols as well as the mechanism of polymerization depend on the nature of monomers, solvent composition, and type of enzyme.[11−13] To increase the processability, thermal stability, and mechanical stability of the polymer, it is desirable to understand both the reaction kinetics and the coupling mechanism, especially during the early stage of the polymerization. It was established that phenols with electron-donating groups as substituents were consumed faster than those with electron-withdrawing groups.[14] Furthermore, the rates of polymerization reaction of para- and meta-substituted phenols are higher compared to those of ortho-substituted phenols. Although the structural characterizations of the polymers obtained from various phenolic monomers have been widely studied,[3] there are limited reports on the nature of coupling in the early stage of the polymerization and the nature and position of the substituents on the mechanism of polymerization. Thus, understanding how the actual phenol coupling takes place during the initial stage of the enzymatic polymerization may have a direct impact on the final structure of the polymer.

[†] University of Massachusetts Lowell.
[‡] U.S. Army Soldier and Biological Chemical Command.

10.1021/ma021142b CCC: $22.00
Published on Web 12/05/2002

High-resolution NMR has been one of the most useful tools for studying the structures of oligomers and polymers along with mechanism of polymerization. However, until now, very few nuclear magnetic resonance (NMR) spectroscopy studies on the mechanism of enzyme-catalyzed polymerization of phenolic monomers have been reported.[15−17] Recent NMR work on understanding the coupling mechanism of the enzymatic polymerization of 8-hydroxyquinoline-5-sulfonate and 4-sulfonated phenol in aqueous medium shows that NMR is a sensitive technique for analyzing the enzymatic coupling of phenolic monomers. In this approach it is possible to know the coupling position on the phenol ring and the progress of the reaction with incremental additions of H_2O_2.

In the present study, we report a detailed structural characterization of enzymatic oxidative polymerization of *p*-cresol (an electron-donating group) in an aqueous−organic media by in-situ ^{1}H NMR spectroscopy. The selection of aqueous−organic media helps to keep the reaction products in the solvent medium. The emphasis is on the study of the coupling mechanism and quantitative estimation of monomer and dimer concentrations during the initial stage of polymerization. The polymerization reaction was monitored with (i) incremental additions of H_2O_2 to the reaction mixture in the NMR tube at a regular interval and (ii) a function of time after the addition of a known amount of H_2O_2. Monitoring the initial stage of reaction by in-situ NMR spectroscopy provides invaluable information on coupling mechanism and polymer formation. 2D ^{1}H−^{1}H gradient-assisted correlation spectroscopy (gCOSY) was used to assign chemical shifts for predominant species formed during the early stage of enzymatic polymerization.

Experimental Section

Materials. Horseradish peroxidase (HRP) (150−250 units/mg of solid) was purchased from Sigma Chemical Co. (St. Louis, MO). A stock solution of 10 mg/mL in pH 7.0, 0.1 M phosphate buffer was prepared. The monomer *p*-cresol and pyrazine (reference standard) were purchased from Aldrich Chemical Co. Inc., Milwaukee, WI, and used as received. All other chemicals and solvents used were of analytical grade and used as received.

In-Situ NMR Measurements. In-situ ^{1}H NMR spectra were recorded on a Bruker DRX-500 MHz NMR spectrometer at ambient temperature with a 5 mm broadband probe. The polymerization reaction was carried out in the 5 mm NMR tube. To a NMR tube, 0.4 mL of acetone-d_6 and 0.1 mL of pH 7.0, 0.01 M phosphate buffer (prepared in D_2O) were added. This was followed by addition of 3 mg of monomer (*p*-cresol), 0.3 mg of HRP, and 0.5 mg of pyrazine to the above solution. The solution was shaken for 5 min, and the initial ^{1}H spectrum was recorded. Experimental conditions for the in-situ NMR study were optimized for acquiring a reasonable signal-to-noise ratio in less than 1 min. Typical operating parameters for ^{1}H NMR experiment were as follows: a 6 kHz spectral width, a 4.4 μs (30° pulse) pulse width, a 1 s acquisition time, a 16K time domain data point, a 2 s relaxation delay, and 16 transients. The data were processed with 0.3 Hz line broadening and twice zero-filled prior to Fourier transformation. The spectrum was internally referenced by assigning the chemical shift of the singlet for pyrazine at 8.7 ppm with respect to tetramethylsilane (TMS). The first ^{1}H NMR spectrum was recorded soon after the addition of 5 μL of H_2O_2 (0.2 M in D_2O) to the NMR tube containing the reaction mixture. A total of 40 μL of H_2O_2 was added in eight increments. Further H_2O_2 addition resulted in the rapid loss of intensity of various resonances due to the precipitation inside the NMR tube. A series of spectra were recorded after each incremental addition of H_2O_2 and calibrated with the height of the internal standard resonance at 8.7 ppm. Areas of each individual resonance were quantitatively measured relative to the area of the internal standard.[17] The 2D gCOSY spectra were obtained using a ^{1}H/^{13}C/^{15}N/^{2}H 5 mm inverse probe equipped with gradient coils. The spectrum was collected with a 6 kHz spectral window in both dimensions, a 0.153 s acquisition time, 2048 data points, a 1.5 s relaxation delay, and a 8.3 μs 90° ^{1}H pulse; one transient was accumulated for each of 128 increments during t_1. The data were processed using a sine bell weighting and twice zero-filled prior to Fourier transformation.

Scheme 1

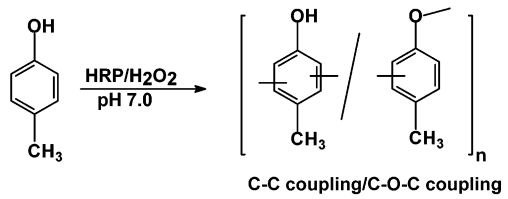

Another series of ^{1}H NMR spectra were recorded at fixed interval of 30 s between each experiment on a similar sample solution immediately after one time addition of 5 μL of H_2O_2 (0.2 M D_2O). The experiment was then allowed to continue for 75 min, and a total of 150 spectra were recorded to study the kinetics of the in-situ polymerization reaction. The experimental parameters for this set of data remained the same as described above except for a 1 s relaxation delay and 8 transients per spectrum.

Enzymatic Polymerization. The peroxidase-catalyzed polymerizations of *p*-cresol were carried out at room temperature in a volume of 100 mL in a 250 mL beaker. A typical initial mixture prior to polymerization contains 0.1 M, pH 7.0 sodium phosphate buffer solution and acetone in equal volume along with *p*-cresol (0.54 g, 5 mM) and HRP (10 mg). The reaction was initiated by addition of a stoichiometric amount of H_2O_2 under constant stirring. To avoid the inhibition of HRP due to excess of H_2O_2, a dilute solution of H_2O_2 was added in small increments (3 μL) over a period of 2 h into the reaction mixture. After a final incremental step addition of H_2O_2, the reaction mixture was stirred overnight under ambient conditions. The precipitate was then filtered and washed thoroughly with an acetone−water mixture to remove trapped monomer and enzyme. The resulting solution was dried at room temperature, and the powder sample was vacuum-dried for another 24 h. The polymer obtained was then again stirred in 30 mL of methanol to remove oligomers and low molecular weight byproducts. The mixture was then filtered with repeated washing, and the residue was dried in a vacuum for 24 h. The filtrate was also collected after evaporation of methanol, vacuum-dried, and stored.

Polymer Characterization. Structural characterizations of the poly(*p*-cresol) and the reaction products were carried out using ^{1}H and ^{13}C NMR and FT-IR spectroscopy. ^{1}H and ^{13}C NMR spectra were recorded on a Bruker DRX-500 MHz NMR spectrometer operating at 500.13 MHz for ^{1}H and 125.77 MHz for ^{13}C. The samples were prepared by dissolving the polymers in a 0.6 mL of dimethyl sulfoxide (DMSO-d_6) or in a mixture of dimethylformamide (DMF-d_6) and DMSO. A ^{13}C DEPT 90 spectral editing experiment was also carried out for the assignment of various aromatic resonances (to distinguish protonated from nonprotonated carbon). The molecular weight distribution of the poly(*p*-cresol) was measured using a Bruker reflex MALDI−TOF (matrix-assisted laser desorption ionization time-of-flight) mass spectrometer. Calibration of the mass spectrometer was performed using polystyrene standard, and dithranol was used as a matrix for the sample measurement.

Results and Discussion

A generalized oxidative coupling of *p*-cresol is shown in Scheme 1. Two kinds of couplings are possible: (a) a C−C coupling to form phenylene units and (b) a C−O−C

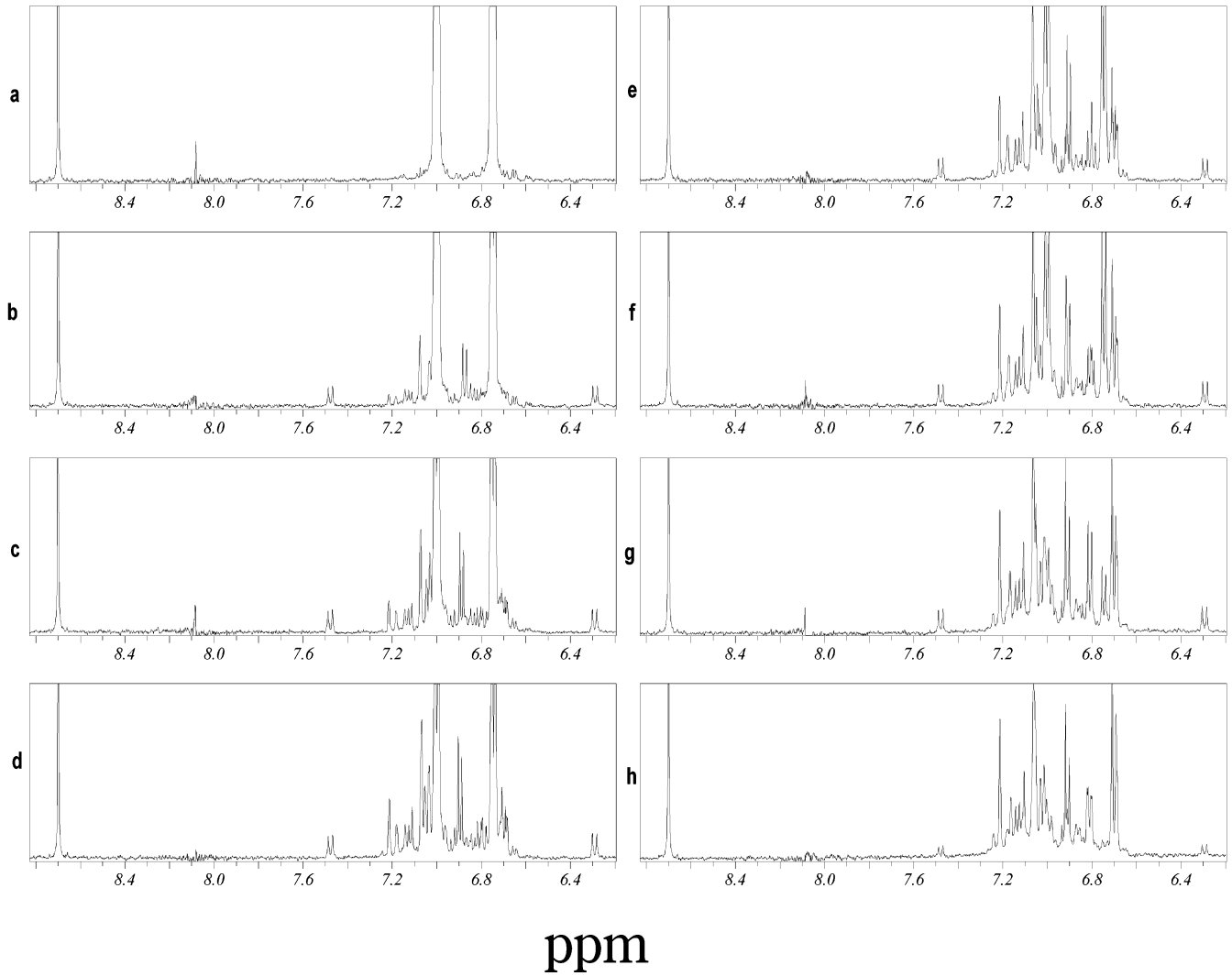

Figure 1. Stacked plot of ^{1}H NMR spectra of the aromatic region of the enzymatic polymerization of *p*-cresol with each incremental addition of H_2O_2: (a) monomer; (b) 5 μL of H_2O_2; (c) 10 μL of H_2O_2; (d) 15 μL of H_2O_2; (e) 20 μL of H_2O_2; (f) 25 μL of H_2O_2; (g) 30 μL of H_2O_2; (h) 35 μL of H_2O_2.

coupling to form oxyphenylene units.[18] The nature of coupling in phenol and substituted phenols during HRP-catalyzed enzymatic polymerization depends largely on the nature of substrate and the reaction medium. The ratio of phenylene and oxyphenylene repeating units is dependent on the nature of substituents.[19] Figure 1 shows a stack plot of vertically expanded in-situ ^{1}H NMR spectra (6.0−9.0 ppm) recorded after each incremental addition of 5 μL of H_2O_2. All the resonances in the ^{1}H NMR spectra are normalized with the internal standard (pyrazine) peak at 8.7 ppm. Pyrazine, a symmetric molecule (chemically inert in this reaction medium), was used as an internal standard to obtain quantitative information on the conversion of monomer and oligomer during the early stage of the polymerization.[17] The monomer spectrum in Figure 1a shows two doublets at 6.75 and 7.0 ppm due to the ortho and meta protons, respectively. The resonance due to the methyl protons appears at 2.21 ppm as a singlet (Figure 2). The −OH proton was not observed in the ^{1}H NMR spectra due to deuterium exchange with the solvent (D_2O).

The reaction was initiated soon after the initial addition of 5 μL of H_2O_2, as observed by the decrease of the monomer peak intensity with respect to the pyrazine resonance at 8.7 ppm in the ^{1}H NMR spectrum (Figure

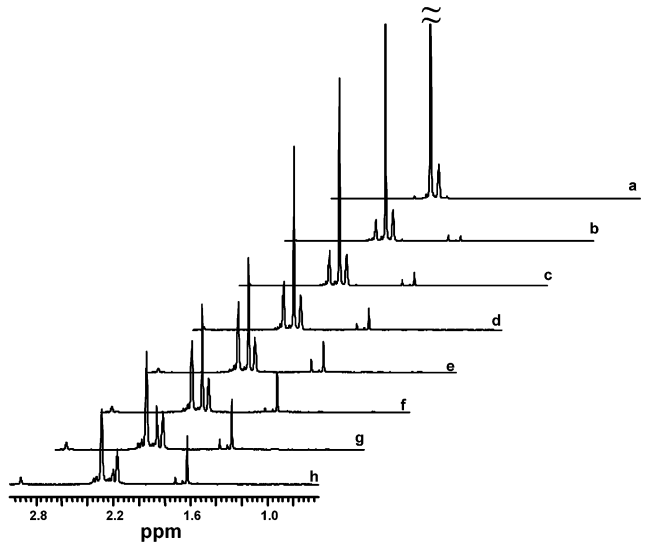

Figure 2. Stacked plot of ^{1}H NMR spectra of the aliphatic region of the enzymatic polymerization of *p*-cresol with each incremental addition of H_2O_2: (a) monomer; (b) 5 μL of H_2O_2; (c) 10 μL of H_2O_2; (d) 15 μL of H_2O_2; (e) 20 μL of H_2O_2; (f) 25 μL of H_2O_2; (g) 30 μL of H_2O_2; (h) 35 μL of H_2O_2.

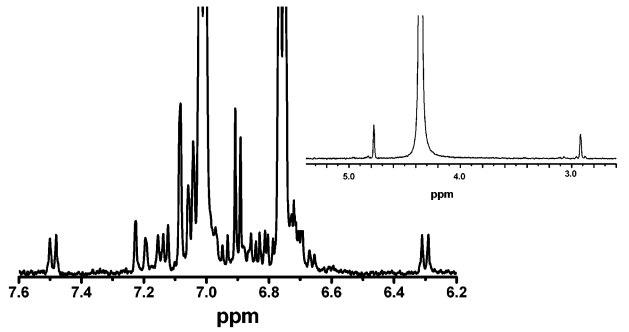

Figure 3. Vertically expanded ^{1}H NMR spectrum of the reaction mixture of the enzymatic polymerization of *p*-cresol after addition of 5 μL of H_2O_2 (inset showing the region of 2.6−5.4 ppm).

1b). The reaction mixture changed from colorless to yellowish brown after the initial addition of H_2O_2. In addition, new resonance peaks are observed in the 6.2−7.6 ppm region. For better visualization of these new resonances, a vertically expanded ^{1}H NMR spectrum of an intermediate stage of the in-situ polymerization is presented in Figure 3. Prominent resonances representing the oligomeric aromatic protons at the initial stage of the reaction (after addition of 5 μL of H_2O_2) appear as a singlet at 7.09 ppm and three doublets at ca. 6.30, 6.90, and 7.49 ppm (Figures 1b and 3). Other than these resonances, some weaker resonances also appeared as overlapped multiplets in the 6.63−6.73, 6.80−6.87, and 7.12−7.24 ppm regions. The relative intensities of new resonances are weak compared to the monomer resonances, indicating the presence of a low concentration of oligomers in the reaction mixture at the early stage of polymerization. In the subsequent spectra recorded after successive additions of H_2O_2, the intensity of monomer resonances decreased gradually, and new resonances for various oligomeric products in the reaction mixture increased. As a result, an overall complex spectral pattern is observed in the 6.6−7.3 ppm region. After the addition of 20 μL of H_2O_2, a hump representing a broader distribution of oligomeric species appears in the aromatic region (6.6−7.3 ppm), and its area increases with subsequent incremental additions of H_2O_2 (Figure 1e−h).

Scheme 2 illustrates the presence of possible phenoxy radicals and the most probable coupling modes to form dimers during the polymerization of *p*-cresol. There are three possibilities, i.e., an ortho C−O−C coupling to form dimer (structure **8**), an ortho−ortho C−C coupling to form dimer (structure **9**), and an ortho−para C−C coupling to form dimer (structure **7**). The gradual decrease of monomer resonances (6.75 and 7.0 ppm) with incremental addition of H_2O_2 shows the conversion of monomer to form dimers and oligomers. Among the various multiplets, two resonances at 6.90 (doublet) and 7.09 ppm (singlet) are the intense peaks in the early stage of the reaction (Figures 1b and 3). The $-CH_3$ resonance peak appears at 2.20 ppm in the monomer spectrum (Figure 2a). After the initial addition of H_2O_2, a strong resonance appears at 2.28 ppm, and the intensity of this resonance peak increases with incremental amount of addition of H_2O_2 (Figure 2b). These resonances may be due to one of the possible dimers presented in Scheme 2. Because of the complex nature spectral pattern due to overlapping of resonances arising from many reactions products with varying concentration, our emphasis is to focus on the assignment of

Scheme 2

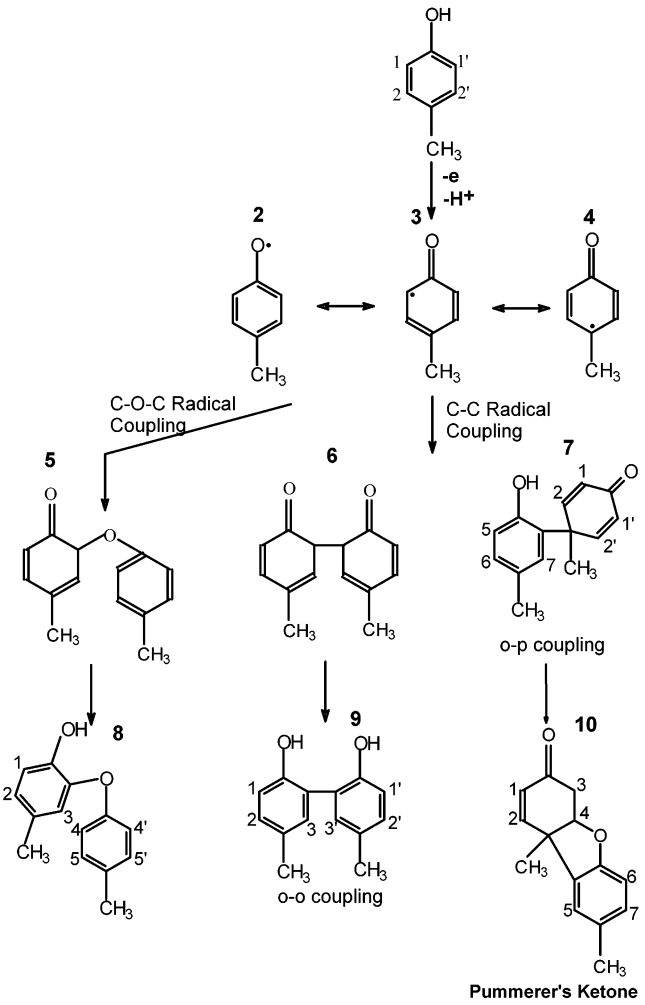

predominant resonances with the aid of model compounds along with the use of spectral simulation software. In addition, 2D correlation NMR was also used to assign some of these resonance peaks in the complex spectrum. Using an inverse probe equipped with gradients, 2D ^{1}H−^{1}H gCOSY experiments were performed at various time intervals during the in-situ polymerization of *p*-cresol. By applying a pulse field gradient (PFG) coherence selection pathway, it is possible to obtain a spectrum by acquiring only one transient per t_1 increment, reducing the experimental time to 3.5 min per 2D data set.

Figure 4 shows the contour maps of the gCOSY experiment at two intermediate stages (after addition of varying amount of H_2O_2 to the reaction mixture) during the in-situ enzymatic polymerization of *p*-cresol. In these contour maps, the diagonal contour shows the 1D ^{1}H NMR spectrum whereas the cross-peaks show connectivity to the coupled protons for species in the reaction mixture. In Figure 4, the cross-peak between the two doublets at ca. 6.90 and 7.04 ppm is a clear indication that these two sets of protons are from the same oligomeric species and coupled to each other. Thus, detailed 1D and 2D NMR data analysis indicates that the two doublets at ca. 6.90 and 7.04 ppm and a singlet at 7.09 ppm are from one oligomeric species. These resonances are tentatively assigned to protons 1, 2, and 3 of the dimer structure **9** in Scheme 2. This inference is based on the splitting pattern, chemical shifts, and indications from the spectral simulation data. Thus,

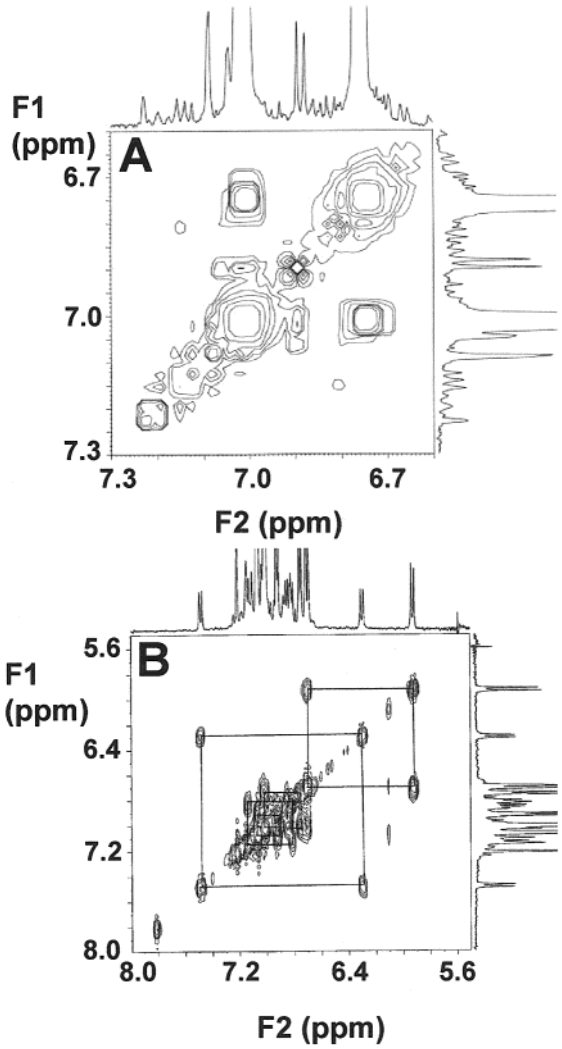

Figure 4. $^1H-^1H$ gCOSY 2D NMR spectra of the intermediate stage of the enzymatic polymerization of *p*-cresol showing aromatic region: (a) 20 μL of H_2O_2; (b) 40 μL of H_2O_2.

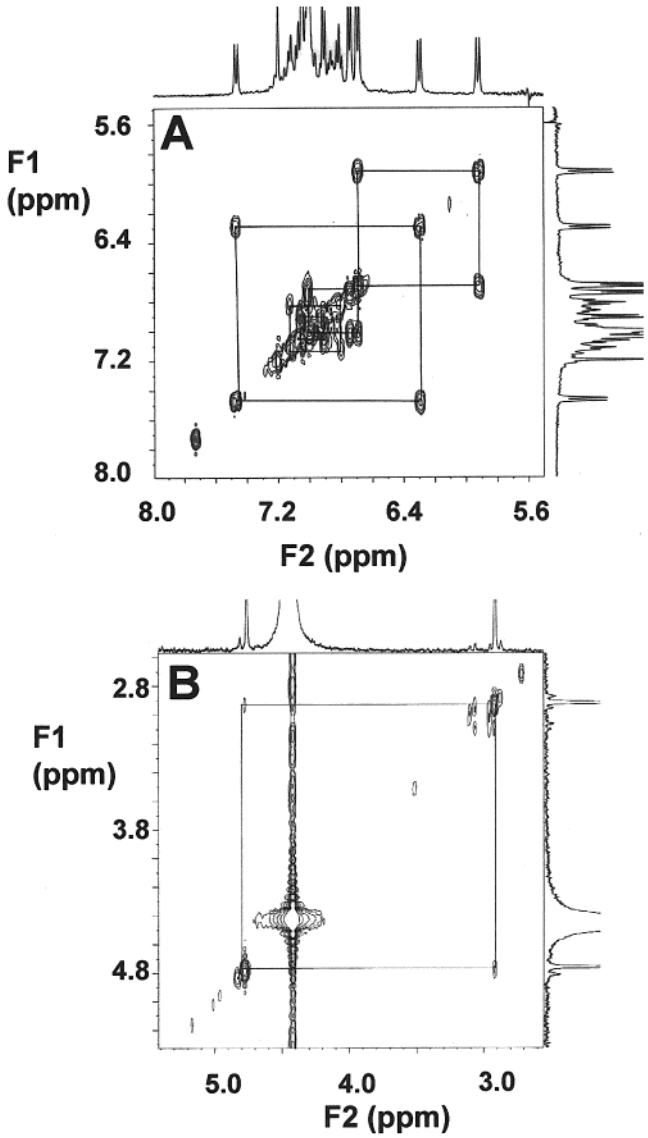

Figure 5. $^1H-^1H$ gCOSY 2D NMR spectra of the enzymatic polymerization of *p*-cresol after 40 min of the reaction time: (a) 5.5−8.0 ppm region; (b) 2.0−6.0 ppm region.

structure **9**, an ortho−ortho C−C coupled dimer, is one of the dominant products at the early stage of the enzymatic polymerization of *p*-cresol. Careful observation indicates that these resonances (6.90 and 7.09 ppm) decreased during the course of polymerization (>30 μL of H_2O_2), suggesting the conversion of the ortho−ortho C−C dimers to high molecular weight oligomers.

There are other three significant observations in the NMR data. First, unlike the above observation, the relative intensities of the two doublets at 6.30 and 7.49 ppm along with a few other resonances (1.71, 6.83, and 6.96 ppm) in the aliphatic and aromatic region (Figures 1 and 2) remained the same up to the addition of 30 μL of H_2O_2. The further addition of H_2O_2 resulted in the decrease of these resonances in the ^1H NMR spectra and finally disappeared after the equimolar addition of H_2O_2 to the reaction mixture (40 μL). Note that these resonances reappeared with the further addition of monomer and H_2O_2 to the reaction mixture after complete consumption of the initial monomer content. This observation suggests that the oligomeric species corresponding to these resonances are consumed during the reaction and may be assigned to quinone type intermediate products (see below). The gCOSY contour plot in Figure 5 shows the presence of distinct cross-peaks between the two doublets at 6.30 and 7.49 ppm. The presence of corresponding methyl resonance at 1.71 ppm indicates that it is no longer bonded to the aromatic ring carbon (methyl attached to aromatic ring appears downfield, >2−3 ppm). Considering the resonances, two doublets (6.30 and 7.49 ppm) and a singlet (1.71 ppm) from the same dimer species, the spectral analysis indicates that these resonances are from the dimer shown in structure **7** (Scheme 2). This is a quinine species formed by the ortho−para C−C coupling. However, to understand the consumption of this quinine dimer species (structure **7**), in-situ ^1H NMR studies of enzymatic polymerization were carried out as a function of reaction time after a known amount of addition of H_2O_2. Detailed aspects of this study are discussed in the later part of this section.

Second, as the quinone resonance of structure **7** decreased, a set of new resonances at 5.92, 6.69, and 7.20 ppm became pronounced in the later stage of the reaction when added H_2O_2 was >20 μL (Figure 3). These resonances were not observed in the spectrum obtained after the addition of 5 μL of H_2O_2 (Figure 1b). The cross-peaks for the doublets at 5.92 and 6.69 in the gCOSY contour map (Figure 5) suggest that these protons are

coupled to each other. In addition, the intensity of the resonance peak at 1.61 ppm increased simultaneously and has a comparable intensity with the peak at 2.28 ppm after the equimolar addition of H_2O_2. The relative area of the methyl resonance peak at 1.61 ppm to that of two doublets at 5.92 and 6.69 ppm indicates that these aromatic doublets correspond to one proton each. Other prominent peaks that may be categorized with these resonances are appeared as singlet at 2.9 and 4.75 ppm (inset in Figure 3). These two peaks also showed the cross-peaks in the gCOSY contour plot; however, the contour intensity is weak compared to that of cross-peaks between doublets at 5.92 and 6.69 ppm. These data suggest the formation of dimer corresponding to structure **10** (Scheme 2). The resonance at 4.75 ppm can be assigned to the proton that attached to oxygen and may correspond to H4 (structure **10**, Scheme 2). However, the singlet nature of both resonance peaks at 2.9 and 4.75 ppm and a weak coupling between them may be due to fast exchange of two H3 protons that take part in tautomerization of the ketone (⟩C═O) with $-CH_2-$ to the corresponding enolic form of structure **10** (Scheme 2). The resonances from the aromatic ring protons appear at 6.74 (H6) and 7.00 ppm (H7), which are merged with the monomer in all the spectra and are clearly distinguishable in the spectra where the concentration of the monomer is significantly lower (Figure 1h). The resonance peak at 7.20 ppm due to H5 appeared as a well distinct singlet. This supports the conversion of the quinonoid species (structure **7**) to a stable ketonic species, Pummerer's ketone (structure **10**, Scheme 2). (The presence of ketone is also confirmed from the ^{13}C NMR spectrum of the reaction mixture.)

The other possible dimer structure is structure **8** (Scheme 2), which is through the C−O−C coupling. However, for this structure, four doublets and a singlet, in which two of the doublets must be half the area of other two doublets, are expected. The multiple resonances in the region of 6.75−6.9 and 7.1−7.2 ppm may be assigned to the dimer corresponding structure **8**. The gCOSY contour map in Figure 5 indicates the presence of coupling between protons in the above region. However, because of severe spectral overlapping of resonances in this region, the unequivocal assignments for resonances of this structure is rather challenging with the present experimental setup. However, the relative intensities of these resonances compared to new resonances that appeared during the early stage of reaction suggest that the dimer concentration of the corresponding structure **8** is lower. The formation of oligomers, higher than dimer, in the reaction mixture appeared as a broad hump in the 6.6−7.3 ppm region due to the heterogeneity of chemical shifts arising from the molecular weight distribution of oligomers.

Thus, the present data indicate that the C−C coupling (ortho−ortho and ortho−para coupling) is preferred over the C−O−C coupling during the early stage of enzymatic polymerization of *p*-cresol. This is an interesting observation simply because, in the case of 4-sulfonated phenol, the predominant coupling is through C−O−C coupling whereas in the case of phenol both the C−C and C−O−C coupling are present during the early stage of polymerization.[17,18] It appears that the preference of a particular type of coupling may be related to the nature of substituents in the para position. In the case of 4-sulfonated phenol, the para substituent is an electron-withdrawing $-SO_3H$ group while in the case of *p*-cresol, $-CH_3$ is an electron-donating group and may have a role in the radical coupling mechanism whereas there are no para substituents in phenol. The latter shows no preferences to either C−C or C−O−C coupling.[19]

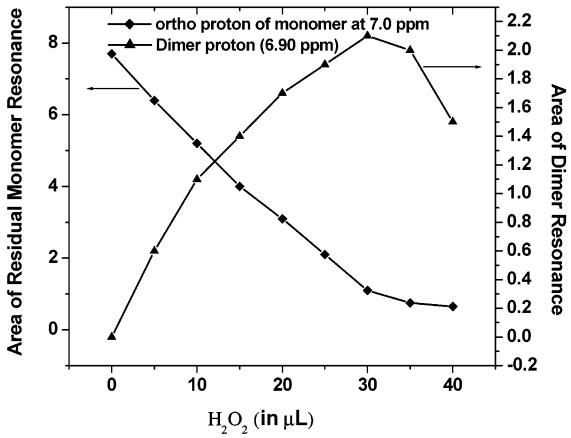

Figure 6. Plots showing the concentration of residual ortho and meta protons of monomer as a function of H_2O_2 addition. Also shown is the variation in the integrated area of dimer resonances as a function H_2O_2 addition.

The decrease of the area of monomer resonance (7.0 ppm) as a function of H_2O_2 is presented in Figure 6. The quantitative analysis of the area of monomer resonance was performed with the internal standard peak, assigning the area of the internal standard (8.7 ppm) resonance to a unit value each time.[17] Up to 30 μL of H_2O_2, the monomer resonance decreases linearly and almost 90% of the monomer resonances disappear during this period. Further additions of H_2O_2 show only a slight decrease of the monomer resonance. The quantitative analysis of the C−C dimer contents in the reaction mixture as a function of H_2O_2 was measured by quantifying the area of the doublet at 6.90 ppm (H1and 1′, structure **9**) and is presented in Figure 6. The dimer concentration increased up to 30 μL of H_2O_2 and then decreased there after. This result shows that the dimer concentration in the solution increases during initial stage of the polymerization in proportion with the decrease of monomer. Figure 6 also suggests that the consumption of the C−C dimer begins when the monomer concentration decreases to a minimum level. Initially, oxidative coupling of monomer radicals resulted in the formation of dimers. At subsequent addition of H_2O_2 to a total of 30 μL, it appears that dimers continue to be formed. If the dimers continued to be formed without being consumed, then a linear response for the curve showing the area of dimer resonance is expected in Figure 6. Deviation from the linear response after addition of 10 μL of H_2O_2 is an indication that dimers are also being consumed during the polymerization process. Significant consumption of dimer takes place only after complete consumption of monomer. At this point, there are abundant ortho−ortho C−C coupled dimers of structure **9**, Scheme 2, with hydroxyl group available to form radicals on them by the enzyme. Further addition of H_2O_2 will initiate the radical formation on these dimers since there are no monomers present in the reaction products. This results in the formation of high molecular weight oligomers. In the case of enzymatic polymerization of 4-sulfonated phenol, three stages of polymerization has been observed, in which a dynamic equilibrium exists in stage II between

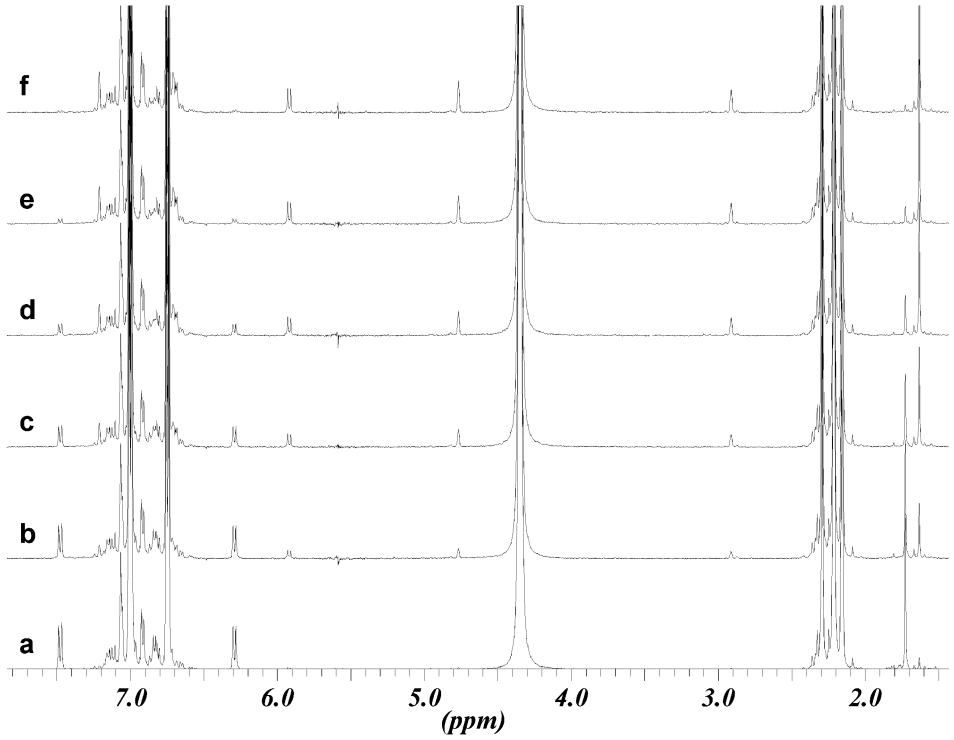

Figure 7. Stacked plot of ^{1}H NMR spectra of the enzymatic polymerization of *p*-cresol as a function of increasing reaction time after the addition of a fixed amount of H_2O_2: (a) 2.5, (b) 10, (c) 20, (d) 30, (e) 40, and (f) 75 min.

the formation and consumption of the dimers in the reaction system.[17] On the other hand, a similar equilibrium stage exists for phenol; the dynamic equilibrium shifts slightly toward the formation of dimer.[19] This is mostly due to the reactivity of the dimer in the reaction medium. In the present study, the dynamic equilibrium shifts more toward the formation of dimers, thus bypassing the intermediate dynamic equilibrium stage between formation and consumption of dimers.

Monitoring the Polymerization with Time. The reaction mixture turns into a bright yellowish-brown solution after the initial addition of H_2O_2 but slowly fades away to a light yellow color solution with time. The change of color with time of the reaction mixture may be due to the formation of quinone type species as an intermediate product in the polymerization. The presence of quinonoid structure (quinone−ketal) intermediates in the polymerization of phenolic derivatives such as 2,6-dimethylphenol, 4-ethylphenol, 2-naphthol, 4-phenoxyphenol, and 4,4′-dihydroxydiphenyl ether has been identified by various spectroscopic techniques.[20−23] NMR is a sensitive technique to monitor the fate of quinine type species present in the reaction products. ^{1}H NMR spectra were recorded at regular intervals of time after one time addition (5 μL, 0.2 M in D_2O) of H_2O_2 to begin the polymerization (Figure 7). In the aromatic region, two doublets at 6.30 and 7.49 ppm disappear with time along with the 6.85 and 6.97 ppm resonances in the aromatic region and the 1.71 ppm resonance in aliphatic region. These are the only resonances decrease with time while the other prominent peaks remain the same with time in Figure 7. The above results suggest that the quinone type species (structure **7**, Scheme 2) was formed by the ortho−para C−C coupling as a side product.. The area of two doublets at 6.30 and 7.49 ppm as a function of increasing reaction time is plotted in Figure 8. This plot shows an exponential decrease of the quinonoid species with time. Unlike the prior reports

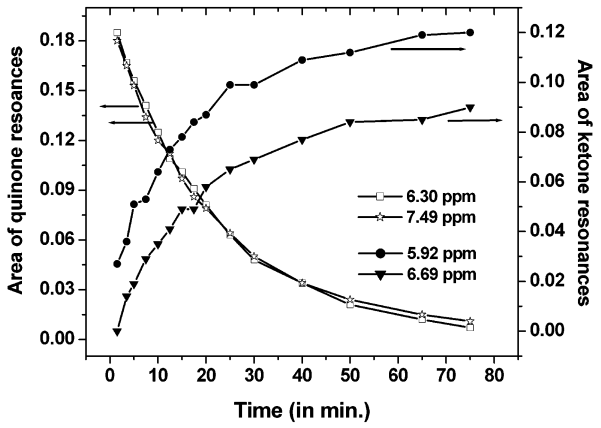

Figure 8. Plots showing the concentration variation of quinonoid protons ortho−para C−C coupled products and protons of Pummerer's ketone as a function of reaction time.

suggesting the presence of intermediate quinonoid species (quinone−ketal intermediate) for the formation of phenolic oligomers during enzymatic polymerization,[21,22] the present work with the NMR results indicates that these quinonoid species are not part of the polymerization reaction to form poly(*p*-cresol). This indicates that the quinone species (structure **7**, Scheme 2) is not an intermediate product (i.e., quinone−ketal intermediate). It is a side product with no active role in the polymerization of *p*-cresol.

However, the absence of quinonoid structures in the in-situ polymerization of sulfonated phenol may be due to the bulky $-SO_3H$ group at the para position with respect to the −OH group. The presence of the bulky $-SO_3H$ sterically hinders the para position from coupling. During the oxidative polymerization of 4-phenoxyphenol by a tyrosinase metal complex catalyst, Higashimura et al.[23] showed the rearrangement and redistribution of quinone−ketal intermediates to form a dimer product in which the para position of phenoxyl

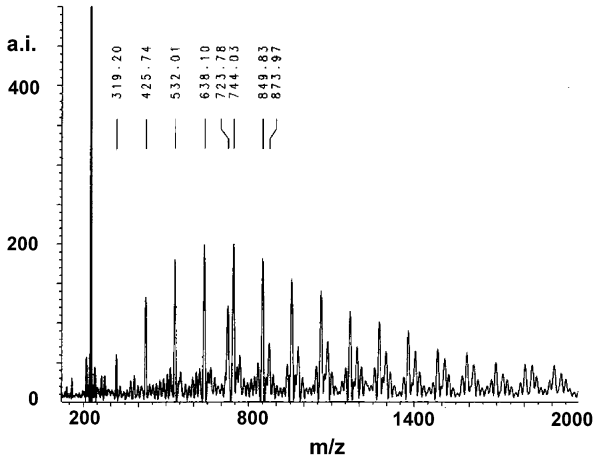

Figure 9. MALDI−TOF mass spectrum of the poly(*p*-cresol) using dithranol matrix.

ring coupled to the C−O of the phenol to form a 1,4-addition product. In contrast, in the polymerization of *p*-cresol, it appears the quinonoid species (structure **7**, Scheme 2) rearranges to form a ketonic species such as Pummerer's ketone (structure **10**, Scheme 2). The decrease in intensity of the two doublets at 6.30 and 7.49 ppm with time is accompanied by the appearance of two new doublets at 5.92 and 6.69 ppm. The new resonances in the ^{1}H NMR spectrum obtained after 75 min after addition of H_2O_2 supports the formation of Pummerer's ketone (structure **7**, Scheme 2). The exponential increase of peak area of these new peaks as a function of time is observed in Figure 8.

The formation of ketonic species (Pummerer's ketone) in peroxidase-catalyzed polymerization of *p*-cresols is known and appears to be the major product along with the ortho−ortho C−C dimer.[18,24−26] The previously reported data suggest that at low concentration of enzyme Pummerer's ketone predominates, but as the enzyme concentration increases, the biphenol product (structure **9**, Scheme 2) is favored.[26] In other studies, it is reported that Pummerer's ketone is the major product formed in the aqueous media, but it is not the case in the organic media. The ortho−ortho C−C coupled dimers (structure **9**) are the major low molecular weight products in the organic medium.[18] The present in-situ ^{1}H NMR studies unambiguously show the formation of the quinonoid species by ortho−para C−C coupling to Pummerer's ketone with time. NMR data suggest that the ketonic species do not participate in the polymerization and remained as side products. However, in recent studies Premachandran et al.[20] showed that the ketonic species formed during the enzymatic polymerization of *p*-ethylphenol and may be either a part of the backbone or possibly an end group.

Characterization of Poly(*p*-cresol) Separated from the Reaction Products. Recently, it has been demonstrated that matrix-assisted laser desorption ionization−time-of-flight mass spectrometry (MALDI−TOF-MS) is a potential tool for studying the presence of oligomers during enzymatic polymerization of phenolic monomers.[27] Figure 9 shows the MALDI−TOF MS of the extracted polymer, extd-poly(*p*-cresol). The number-average molecular weight M_n is 990, and the weight-average molecular weight M_w is 1230 with a polydispersity index (PDI) of 1.24. The peak-to-peak separation is 106, which is the molecular weight of the repeat unit. However, it may be a difficult task by MALDI−TOF-MS to distinguish the nature of coupling, and thus a detailed NMR analysis of the monomer and polymer is carried out.

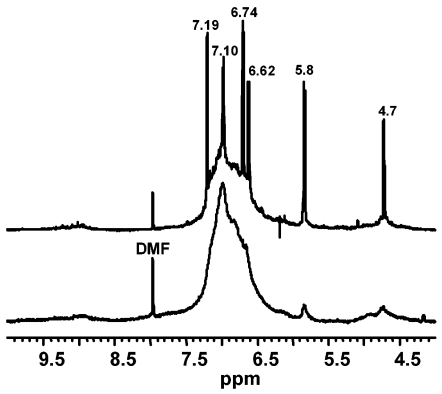

Figure 10. ^{1}H NMR spectra of the poly(*p*-cresol) before (a) and after extraction with methanol (b).

The ^{1}H NMR spectra of the reaction product from enzymatically prepared poly(*p*-cresol) before and after extraction from the methanol solvent are shown in Figure 10. The appearance of a broad featureless hump, a characteristic of polydispersed high molecular weight products, indicates the formation of poly(*p*-cresol). However, sharp peaks overlapped with the broad hump are visible in Figure 10a. These sharp peaks are due to Pummerer's ketone (structure **10**, Scheme 2), which remain as a side product during the enzymatic polymerization. Note that the peaks at 6.74 and 7.10 are not due to monomer, but due to the protons 5 and 6 (structure **10**, Scheme 2). The ^{1}H NMR spectrum after extraction (Figure 10b) shows the disappearance of low molecular weight oligomers and Pummerer's ketone which results in a single broad hump in the aromatic region. However, a few residual broad signals are observed at 4.7 and 5.8 ppm, indicating the presence of Pummerer's ketone as part of the polymer chains, possibly as an end group, which supports the observations by Premchandran et al.[20] The broadness of these very weak resonances is an indication that the low molecular weight side products are absent after extraction.

The ^{13}C NMR spectra of *p*-cresol and poly(*p*-cresol) before and after extraction from methanol along with a DEPT 90 spectrum of extd-poly(*p*-cresol) are shown in Figure 11. The larger chemical shift range of the ^{13}C NMR spectrum results in an enhanced spectral resolution of different species, which helps in the assignment of various carbons. The monomer *p*-cresol shows four distinct resonances in the aromatic region at 115 (C2, C6), 129 (C4), 130 (C3, C5), and 155 ppm (C1) (Figure 11a). The methyl resonance appears at 20 ppm in the aliphatic region (not shown in Figure 11). After polymerization, the ^{13}C NMR spectrum shows a number of additional sharp peaks along with a broad distribution of chemical shifts at 115−140 and 146−158 ppm. The sharp peaks are due to the isolated Pummerer's ketones in the polymerization products (Figure 11b). The absence of monomer resonances is clearly visible by comparing the monomer and polymer spectra (Figure 11a,b), indicating the disappearance of the resonance at 115 ppm (ortho carbon of the monomer) in the polymer spectrum. The ^{13}C NMR spectrum of the extracted polymer, extd-poly(*p*-cresol), is shown in Figure 11c. The spectral feature of this polymer sample

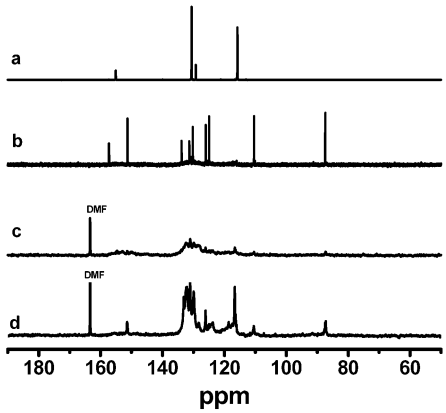

Figure 11. ^{13}C NMR spectra of the monomer (a) and the poly(*p*-cresol) before (b) and after extraction with methanol (c) and its DEPT 90 spectrum (d). The structures of the monomer and polymer unit are shown with possible assignments.

shows the absence of isolated Pummerer's ketone. Comparing the ^{13}C NMR spectrum with the DEPT 90 spectrum (only protonated ^{13}C NMR resonances appear in this spectrum) (Figure 11d), it is clear that C−C coupling is one of the dominant mechanisms in the polymerization process. The disappearance of the 129 ppm resonance in the DEPT 90 spectrum indicates the presence of C−C coupled carbons. In addition, the broad distribution of C−OH carbons in the 146−158 ppm region in Figure 11c shows that not all the −OH groups take part in the polymerization. The presence of residual Pummerer's ketone as an end group is also indicated by the presence of resonances at 87.0, 111.0, and 151.0 ppm. The 151 ppm resonance, which is due to =CH carbon (C3), is present in the DEPT 90 spectrum.

Conclusions

For the first time, the in-situ 1D and 2D NMR analysis of enzymatic polymerization in a mixed solvent medium with various experimental approaches (with incremental H_2O_2 addition as well as the function of reaction time with a fixed amount of H_2O_2) was used to monitor the course of the enzymatic polymerization. The combined 1D and 2D NMR analysis suggests the ortho−ortho C−C coupling as the major coupling mechanism during the initial stage of the polymerization. The quantitative NMR analysis indicates that the relative consumption of monomer is higher than the dimer and the dimer consumption significantly increases only after complete consumption of monomer from the reaction mixture. The in-situ NMR analysis as a function of reaction time after a fixed addition of H_2O_2 suggests the formation of a quinonoid intermediate by ortho−para C−C coupling, which readily converts to Pummerer's ketone. For the first time we unambiguously assigned resonances for the quinonoid and ketonic species. Structural characterization of the bulk polymer synthesized by biocatalytic means, poly(*p*-cresol), using multinuclei NMR and MALDI−TOF mass spectrometry indicates the formation of high molecular weight polymers (M_w 1230) and the dominance of ortho−ortho and ortho−para C−C coupled products. Further, the detailed structural analysis of the extracted bulk poly(*p*-cresol) suggests the presence of Pummerer's ketone in residual amounts as chain ends in the C−C coupled polymer chain.

Acknowledgment. The support of this research by the National Science Foundation (NSF Grant DMR-9986644) is greatly acknowledged. The authors thank Prof. V. S. Parmar, Dr. F. F. Bruno, Dr. Ravi Mosurkal, and Mr. Jeffery Njus for many helpful suggestions during the course of this work. We thank Mr. Peng Xu for his help in recording MALDI−TOF MS data and Prof. David Kaplan, Tufts University, for the use of their MALDI−TOF MS research facilities.

References and Notes

(1) Dordick, J. S.; Marietta, M. A.; Klibanov, A. M. *Biotechnol. Bioeng.* **1987**, *30*, 31.
(2) Akkara, J. A.; Senecal, K. J.; Kaplan, D. L. *J. Polym. Sci., Part A: Polym. Chem.* **1991**, *29*, 1561.
(3) Kobayashi, S.; Uyama, H.; Kimura, S. *Chem. Rev.* **2001**, *101*, 3793 and references therein.
(4) Akkara, J. A.; Kaplan, D. L.; John, V. J.; Tripathy, S. K. In *Polymeric Materials Encyclopedia*; Salamone, J. C., Ed.; CRC Press: Boca Raton, FL, 1996; Vol. 3, p 2116.
(5) Uyama, H.; Kobayashi, S. *CHEMTECH* **1999**, *29* (10), 22.
(6) Dunford, H. B. In *Peroxidases in Chemistry and Biology*; Everse, J., Everse, K. E., Grisham, M. B., Eds.; CRC Press: Boca Raton, FL, 1991; Vol. 2, pp 1−24.
(7) Ryu, K.; McEldoon, J. P.; Pokora, A. R.; Cyrus, W.; Dordick, J. S. *Biotechnol. Bioeng.* **1993**, *42*, 807.
(8) Uyama, H.; Kurioka, H.; Kaneko, I.; Kobayashi, S. *Chem. Lett.* **1994**, 423.
(9) Mandal, B. K.; Walsh, C. J.; Sooksimuang, T.; Behroozi, S. J. *Chem. Mater.* **2000**, *12*, 6.
(10) Liu, W.; Bian, S.; Li, L.; Samuelson, L.; Kumar, J.; Tripathy, S. *Chem. Mater.* **2000**, *12*, 1577.
(11) Uyama, H.; Kurioka, H.; Sugihara, J.; Kobayashi, S. *Bull. Chem. Soc. Jpn.* **1996**, *69*, 189.
(12) Uyama, H.; Kurioka, H.; Sugihara, J.; Komatsu, I.; Kobayashi, S. *J. Polym. Sci., Part A: Polym. Chem.* **1997**, *35*, 1453.
(13) Tonami, H.; Uyama, H.; Kobayashi, S.; Kubota, M. *Macromol. Chem. Phys.* **1999**, *200*, 2365.
(14) Xu, Y.-P.; Huang, G.-L.; Yu, Y.-T. *Biotechnol. Bioeng.* **1995**, *47*, 117.
(15) Alva, K. S.; Marx, K. A.; Kumar, J.; Tripathy, S. K. *Makromol. Rapid Commun.* **1997**, *18*, 133.
(16) Alva, K. S.; Samuelson, L. A.; Kumar, J.; Tripathy, S. K.; Cholli, A. L. *J. Appl. Polym. Sci.* **1998**, *70*, 1257.
(17) Liu, W.; Cholli, A. L.; Kumar, J.; Tripathy, S.; Samuelson, L. *Macromolecules* **2001**, *34*, 3522.
(18) Pietikaeinen, P.; Adlercreutz, P. *Appl. Microbiol. Biotechnol.* **1990**, *33*, 455.
(19) Sahoo, S. K.; Liu, W.; Samuelson, L.; Kumar, J.; Cholli, A. L. *ACS Symp. Ser.*, in press.
(20) Premchandran, R.; Banerjee, S.; Wu, X.-K.; John, V. T.; McPherson, G. L.; Akkara, J. A.; Ayyagari, M.; Kaplan, D. L. *Macromolecules* **1996**, *29*, 6452.
(21) Fukuoka, T.; Tonami, H.; Maruichi, N.; Uyama, H.; Kobayashi, S. *Macromolecules* **2000**, *33*, 9152.
(22) Baesjou, P. J.; Driessen, W. L.; Challa, G.; Reedijk, J. *Macromolecules* **1999**, *32*, 270.
(23) Higashimura, H.; Kubota, M.; Shiga, A.; Fujisawa, K.; Morooka, Y.; Uyama, H.; Kobayashi, S. *Macromolecules* **2000**, *33*, 1986.
(24) Westerfield, W. W.; Lowe, C. *J. Biol. Chem.* **1942**, *145*, 463.
(25) Hewson, W.; Donald, D.; Brian, H. *J. Biol. Chem.* **1976**, *251*, 6043.
(26) Celik, A.; Cullis, P. M.; Reven, E. L. *Arch. Biochem. Biophys.* **2000**, *373*, 175.
(27) Xu, P.; Kumar, J.; Samuelson, L.; Cholli, A. L. *Biomacromolecules* **2002**, *87*, 191.

MA021142B